International Journal of Environmental Sciences ISSN: 2229-7359 Vol. 11 No. 7, 2025 https://theaspd.com/index.php

# Green Synthesis of Silver Nanoparticles Using Aegle Marmelos Fruit Extract: Characterisation, Antimicrobial, Cytotoxic and Antioxidant Activities

# Pillala Sai Kiran<sup>1</sup>, Y Vimala<sup>2</sup>

<sup>1,2</sup>Dept. of Microbiology & FST, GITAM Deemed to be University, Visakhapatnam-530045, India.

## Abstract

Silver nanoparticles (AgNPs) are renowned for their exceptional chemical stability, electrical conductivity, and potent biological activities. In this study, we report a novel and environmentally friendly green synthesis of AgNPs using aqueous fruit extract of Aegle marmelos, a medicinally important plant that has not been extensively explored for nanoparticle synthesis. The biosynthesized AgNPs exhibited a distinct surface plasmon resonance peak at 474 nm and an average particle size of 12 nm, confirming their nanoscale nature. Advanced characterization techniques such as UV-Vis spectroscopy, XRD, FTIR, and SEM-EDX were employed to elucidate their structural and functional properties. The novelty of this work lies in the first-time use of A.marmelos fruit extract as both a reducing and stabilizing agent for the green synthesis of AgNPs, resulting in nanoparticles with potent multifunctional biological activities. The synthesized AgNPs demonstrated remarkable antibacterial activity, particularly against E.coli (16.23  $\pm$  0.87 mm inhibition zone at 150 µg/mL) and C.glutamicum (12.66  $\pm$  0.41 mm). Additionally, they exhibited significant antioxidant activity (85.67% at 100 µg/mL) and potent anticancer effects against HCT-116 colon cancer cells, with an IC50 of 41.33  $\pm$  0.19 µg/mL. These findings not only establish A.marmelos as a sustainable and effective biogenic source for AgNP synthesis but also highlight the potential of the resulting nanoparticles as promising candidates for biomedical and therapeutic applications.

Keywords: Silver nanoparticles; green synthesis; Aegle marmelos; antimicrobial performance; anticancer activity.

#### 1. INTRODUCTION

Medicinal plants have long been integral to healthcare systems, particularly in traditional practices such as Ayurveda, Siddha, and homeopathy. These systems rely heavily on plant-derived compounds for both therapeutic and preventive treatments. Globally, an estimated 88% of the population continues to depend on plant-based remedies, underscoring the enduring relevance of phytochemicals in modern medicine [1]. The therapeutic potential of medicinal plants stems largely from their secondary metabolites such as flavonoids, alkaloids, terpenoids, and tannins which serve as natural defense compounds against pathogens and environmental stressors [2]. These bioactive compounds offer several advantages over synthetic drugs, including improved biocompatibility, lower toxicity, and fewer side effects, making them valuable candidates for the treatment of both acute and chronic health conditions [3].

In recent years, the integration of nanotechnology with plant-based therapies has opened new avenues in biomedical research. Among various nanomaterials, silver nanoparticles (AgNPs) have garnered significant interest due to their outstanding biological properties, including antibacterial, antifungal, antiviral, anti-inflammatory, and anticancer activities. While conventional chemical and physical methods of nanoparticle synthesis are effective, they often involve toxic reagents, high energy consumption, and environmental hazards [4–6]. As a sustainable alternative, green synthesis methods utilizing plant extracts have gained prominence. These eco-friendly approaches leverage the reducing and stabilizing capabilities of phytochemicals, enabling the formation of nanoparticles without harmful by-products. Furthermore, green-synthesized nanoparticles often exhibit enhanced biological activity and compatibility, making them suitable for medical applications. Numerous studies have successfully synthesized AgNPs using extracts from medicinal plants such as Acacia concinna, Syzygium cumini, and Emblica officinalis, demonstrating the feasibility and efficiency of plant-mediated nanoparticle production [7]. This green approach not only aligns with sustainable practices but also expands the biomedical utility of AgNPs in areas like drug delivery, wound healing, and antimicrobial coatings.

Previous research has explored the use of methanolic fruit extracts of Aegle marmelos, a plant known for its hepatoprotective, anti-diabetic, anti-diarrheal, and radioprotective properties in the synthesis of AgNPs [8–10]. The integration of A.marmelos extract in green synthesis aligns with the growing demand for nontoxic and sustainable nanomaterials. AgNPs produced via this method benefit from high surface area to

<sup>\*</sup>correspondence email: shaunsaikiran@gmail.com; vyapadin@gitam.edu

Vol. 11 No. 7, 2025 https://theaspd.com/index.php

volume ratios, exceptional chemical and thermal stability, and excellent electrical conductivity, enhancing their performance in biomedical settings. Their potent antibacterial effect is largely attributed to the release of silver ions, which disrupt microbial cell membranes and interfere with essential cellular functions, ultimately leading to cell death [11–12]. Additionally, AgNPs exhibit strong antioxidant properties by neutralizing reactive oxygen species (ROS), which are implicated in oxidative stress and the progression of chronic diseases such as cardiovascular and neurodegenerative disorders [13]. In oncology, AgNPs have emerged as potential adjuvants to conventional chemotherapy, offering the possibility of improved efficacy and reduced side effects.

Given these multifaceted biological activities, AgNPs are increasingly viewed as promising agents for combating infections, managing oxidative stress, and supporting cancer therapy. This study focuses on the green synthesis of AgNPs using the aqueous fruit extract of A.marmelos and explores their antibacterial, antioxidant, and anticancer potential. The research aims to contribute to the growing body of knowledge on plant based nanotechnology and its applications in modern medicine, while offering insights into the clinical viability of AgNPs synthesized through sustainable methods.

## 2. MATERIALS AND METHODS

# 2.1 Chemicals and reagents

The necessary Aegle marmelos fruits were gathered from local homes in Visakhapatnam, India and authenticated by local taxonomist. Silver nitrate ( $AgNO_3$ ) and mercury chloride ( $HgCl_2$ ) of analytical grade were obtained from Himedia, India. We promptly cleaned with tap water to get rid of dust, and then were disinfected with  $HgCl_2$ , as seen in Fig. 1. Finally, we crushed after being further dried at room temperature in a cleaning room. They were then ground into a powder using a kitchen mixer and sieved using an ASTM (American Standard Testing Material) sieving kit.





Fig.1: Fruits of Aegle marmelos

## 2.2 Preparation of fruit extract

Ten grams of finely sieved Aegle marmelos fruit powder were accurately weighed and transferred into a pre-cleaned 250 mL beaker. To this, 200 mL of double-distilled water was added, and the mixture was heated at 60 °C for 1 hour to facilitate the extraction of bioactive compounds [8]. After heating, the solution was allowed to cool to room temperature and subsequently filtered using Whatman No.1 filter paper to remove particulate matter. The clear filtrate, referred to as the fruit extract, was collected in a volumetric flask (Figure 2). To prevent photodegradation, the extract was wrapped in aluminium foil and stored at 4 °C in a refrigerator until further use.

## 2.3 Synthesis of Silver nanoparticles

Silver nitrate (AgNO<sub>3</sub>) served as the precursor for the synthesis of silver nanoparticles (Ag-NPs) [10]. A 0.1 mM aqueous solution of AgNO<sub>3</sub> was prepared, and 75 mL of this solution was mixed with 25 mL of Aegle marmelos fruit extract at room temperature, maintaining a final concentration of 0.1 mM. Within two minutes of mixing, the solution exhibited a visible color change from colorless to dark yellow, indicating the initiation of nanoparticle formation. The color further intensified to dark brown within

https://theaspd.com/index.php

five minutes, suggesting the progressive reduction of silver ions. The successful synthesis of Ag-NPs was confirmed by UV-Visible spectroscopy, which detected the characteristic surface plasmon resonance. The resulting nanoparticles were isolated by centrifugation at 4,000 rpm for 20 minutes. The obtained pellets were washed multiple times (three to four cycles) with distilled water to remove residual organic compounds from the plant extract. After each wash, centrifugation was repeated under the same conditions. The final pellet was carefully collected using a watch glass and dried in a hot air oven at 60 °C for further characterization.



Fig.2: Preparation of fruit extract from A.marmelos

## 2.4 Characterization of AgNP

In this work, the spectrum was observed in the wavelength range of 200–800 nm using a LabIndia UV-3092 UV-Vis spectrophotometer. To determine which functional groups were in charge of stabilizing and reducing the silver nanoparticles, FTIR analysis was performed. At a resolution of 4 cm<sup>-1</sup>, the FTIR spectrum was captured between 4000 and 500 cm<sup>-1</sup>. The X'Pert Pro X-ray diffractometer (D8 Bruker) was used to measure the AgNP crystalline size. The green-synthesised AgNP were subjected to elemental analysis using EDX in conjunction with Scanning Electron Microscopy (SEM JEOL). To assess the stability of the aqueous solution of AgNP, the zeta potential was measured using a Houbara zeta potential analyzer.

## 2.5 Antibacterial activity

The agar well diffusion method was used to assess the isolated compound's antibacterial efficacy against different bacterial strains. Using this technique, the compound's minimum inhibitory concentration (MIC) to stop bacterial growth was also ascertained. The antibacterial activity tests were conducted using bacterial cultures of Pseudomonas aeruginosa (MTCC-2295), Corynebacterium glutamicum (MTCC-2745), Staphylococcus aureus (MTCC-3160), and Escherichia coli (MTCC-443), which were cultured overnight at 37°C.

In a 100 mL conical flask, nutrient agar medium was prepared by dissolving the required amount in distilled water, followed by sterilization in an autoclave at 15 psi for 20 minutes. The sterile medium was then poured into pre-sterilized Petri dishes under aseptic conditions. For antibacterial testing, chloramphenical served as the positive control, while dimethyl sulfoxide (DMSO) was used as the negative control. The antibacterial activity of the synthesized Ag-NPs was assessed using the agar well diffusion method. The surface of the solidified agar plates was uniformly inoculated with the test bacterial strains using a sterilized glass spreader. Five wells were then carefully punched into the agar using a sterile cork borer at equal distances. Ag-NP samples were prepared at final concentrations of 80  $\mu$ g/mL, 100  $\mu$ g/mL, and 150  $\mu$ g/mL. Aliquots of each concentration were dispensed into the respective wells. The plates were incubated at 37 °C for 24 hours. Following incubation, the antibacterial activity was determined by measuring the diameter (in millimeters) of the clear zones of inhibition formed around each well.

International Journal of Environmental Sciences ISSN: 2229-7359 Vol. 11 No. 7, 2025 https://theaspd.com/index.php

# 2.6 Anticancer activity of Ag-NPs

# a. Preparation of HCT-116 cell lines suspension

A subculture of HCT-116 cell lines cultured in Dulbecco's Modified Eagle's Medium (DMEM) was broken down using trypsin. To the broken-up cells in the flask, 50 milliliters of DMEM containing 10% FCS (fetal calf serum) was added. After being carefully pipetted through the liquid to suspend the cells, they were homogenized. Each well of a 24-well growth plate holding one milliliter of the homogenized cell suspension received varying sample concentrations (10 to 200 g/mL). After that, the plate was incubated with 5% CO<sub>2</sub> at 37 °C in a humidified CO<sub>2</sub> incubator. After 48 hours of incubation, the cells were seen under an Olympus x40 magnification inverted tissue culture microscope.

#### b. Cytotoxicity assay

The experiment was carried out using (3,4,5, dimethyl thiazol-2-yl)-2,5-diphenyl tetrazolium bromide (MTT). The mitochondrial succinate dehydrogenase and reductase of living cells convert MTT into detectable purple formazan. This formazan production has a direct correlation with the quantity of viable cells and a negative correlation with the degree of cytotoxicity. MTT was added to the wells following a 48-hour incubation period, and they were then allowed to sit at room temperature for three hours. Each well's contents were extracted using a pipette. After dissolving the formazan crystals with 100 mL of DMSO, each well's absorbance was measured at 540 nm using a Robonik microplate reader. The following Eq. 1 was used to get the percentage growth inhibition .

.% Growth Inhibition = 
$$\frac{\text{OD of Test}}{\text{OD of Control}} \times 100$$
 Eq.(1)

The best biological indicator of cytotoxicity is often determined by the inhibitory concentration 50% ( $IC_{50}$ ). The concentration of the purified substance that resulted in 50% cell inhibition is indicated by the  $IC_{50}$  value.

# 2.7 Anti-oxidant activity of Ag-NPs

The ability of silver nanoparticles (Ag NPs) made from fruit extract from Aegle marmelos to scavenge DPPH (1,1-diphenyl-2-picrylhydrazyl) was assessed. In separate test tubes, different concentrations of the Ag NPs and the standard (ascorbic acid) were produced, ranging from 50 to 150 µg/mL. One milliliter of freshly made DPPH solution (0.3 mM) was added to each test tube, and it was vortexed vigorously. After that, the combinations were left to incubate for half an hour in the dark. Ag NPs were substituted with 2 mL of methanol for the control, which was processed concurrently with the test samples. Using the relevant Eq.2, the AgNP percentage of DPPH radical scavenging activity was determined.

Inhibition 
$$\% = \frac{\text{Absorbance of Control-Absorbance of Test}}{\text{Absorbance of Control}} \times 100$$
 Eq.(2)

# 3. RESULTS AND DISCUSSION

# 3.1 Extracellular synthesis of Ag-NPs

The biosynthesis of silver nanoparticles (AgNPs) using Aegle marmelos fruit extract was successfully demonstrated, as shown in the accompanying images. The aqueous fruit extract, initially light yellowish-brown in color, underwent a noticeable colour change to dark brown (Fig. 3) upon the addition of silver nitrate solution. This colour transition is indicative of the reduction of Ag<sup>+</sup> ions to metallic silver (Ag<sup>0</sup>), mediated by the phytochemicals (Table S1) present in the A.marmelos extract. Such a change is a hallmark of surface plasmon resonance (SPR) associated with the formation of AgNPs. The reaction was conducted under ambient conditions in Visakhapatnam, Andhra Pradesh, as recorded by the GPS tagged photographs. This green synthesis approach highlights the role of naturally occurring reducing and stabilizing agents in plant extracts, offering an eco-friendly, cost-effective, and sustainable route for nanoparticle fabrication without the use of hazardous chemicals [3, 6].



Fig.3: Synthesized Ag NPs using A.marmelos fruit extract

# 3.2 Scanning Electron Microscope analysis

The SEM images of the Ag-NPs synthesized using Aegle marmelos fruit extract, as presented in Fig.4, reveal distinct morphological characteristics at different magnifications at 25000 and 50000x. Fig.4a displays a densely packed aggregation of AgNPs with varied shapes and sizes, indicating a heterogeneous mixture. Fig.4b provides a clearer view of individual nanoparticles. These appear better defined and exhibit relatively uniform morphology, predominantly ribbon-like in shape, suggesting a successful and controlled synthesis process. The enhanced resolution highlights detailed surface features and consistency in particle size, with an average size measured by ImageJ and found to be 40 nm. Table 1 compares the particle sizes of Ag-NPs synthesized using different plant fruit extracts, while Table 2 presents a comparative analysis between Ag-NPs and other metal nanoparticles synthesized using A.marmelos fruit extract.

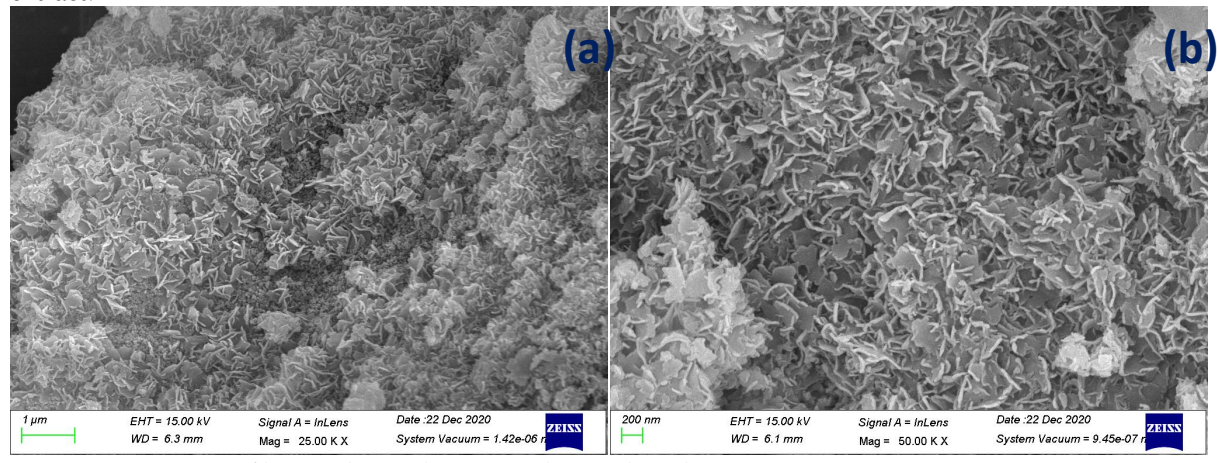


Fig.4: SEM images of biosynthesized A.marmelos-mediated Ag-NPs

Table 1: Size (form SEM) of Ag-NPs using various plant fruit extract

Plant Fruit	Size (nm)	Reference
Aegle marmelos	40	This study
Musa paradisiaca (Banana)	20-50	[7]
Citrus sinensis (Orange)	5-15	[8]
Punica granatum (Pomegranate)	20-40	[29]
Solanum lycopersicum (Tomato)	10-20	[6]
Vitis vinifera (Grape)	10-50	[4]

Vol. 11 No. 7, 2025

https://theaspd.com/index.php

Prunus persica (Peach)	20-60	[25]	
Mangifera indica (Mango)	20-30	[26]	
Carica papaya (Papaya)	10-40	[27]	
Malus domestica (Apple)	15-25	[28]	

# 3.3 UV-Visible spectrum of Ag-NPs

The UV-Visible absorption spectrum of A.marmelos fruit extract-mediated Ag-NPs is illustrated in Figure 5. A distinct surface plasmon resonance (SPR) peak observed at 404 nm confirms the successful formation of AgNPs, which is consistent with previously reported values for Ag NPs [14]. This SPR peak arises from the collective oscillation of conduction electrons at the nanoparticle surface when excited by light and is a characteristic feature of metallic silver at the nanoscale. The sharp and well defined peak at 404 nm suggests a relatively uniform size distribution and spherical morphology of the prepared NPs. The absorbance value at this wavelength, approximately 0.3, indicates a substantial concentration of Ag NPs in the colloidal solution. Furthermore, the spectrum exhibits a broad absorption range between 200 and 600 nm, followed by a gradual decline in absorbance beyond the SPR peak, implying the presence of some polydispersity in the nanoparticle population. Nonetheless, the dominant absorption at 404 nm confirms that nanoscale silver particles are the major constituent of the sample.

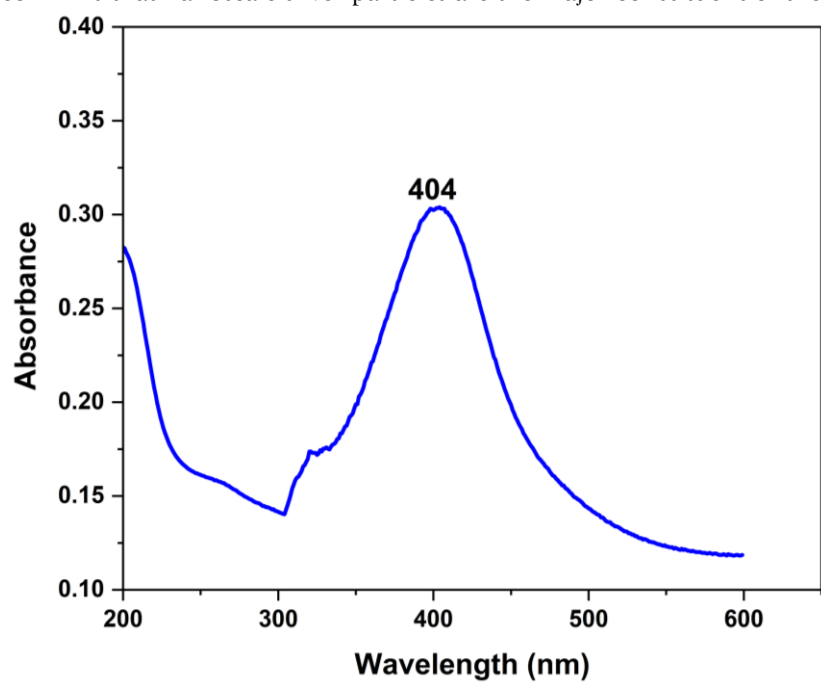


Fig.5: UV-Visible spectrum of biosynthesized Ag-NPs

Table 2: Aegle marmelos fruit extract supported production of different Metal NPs

Nanoparticle	Type	Size (nm)	Properties	Reference
Silver (Ag)	Aegle marmelos fruit extract mixed with silver nitrate solution; heated at 60°C	10-30	Antibacterial activity against E. coli and S. aureus	This study
Silver (Ag)	Aegle marmelos fruit extract mixed with silver nitrate; stirred for 2 hours at room temperature	15-25	Antioxidant and antimicrobial activities	[15]
Gold (Au)	Aegle marmelos fruit extract mixed with chloroauric acid; incubated at 37°C	20-40	Catalytic activity in dye degradation	[16]
Zinc Oxide (ZnO)		30-50	UV-blocking and antibacterial activities	[17]

International Journal of Environmental Sciences ISSN: 2229-7359 Vol. 11 No. 7, 2025 https://theaspd.com/index.php

	zinc acetate; heated at				
	90°C for 3 hours				
Copper (Cu)	Aegle marmelos fruit extract mixed with copper sulfate; stirred	25-35	Antibacterial antioxidant activities	and	[18]

# 3.4 FTIR spectrum analysis of Ag-NPs

The FTIR spectrum of the biosynthesized Ag-NPs, as shown in Figure 6, reveals the presence of various functional groups associated with the biomolecules in the A.marmelos fruit extract that are responsible for both the reduction of silver ions and stabilization of the formed nanoparticles. A broad absorption band at 3441.01 cm<sup>-1</sup> corresponds to the O-H stretching vibrations of phenolic compounds, indicating their involvement in the reduction process [19]. Distinct peaks at 1645.2 cm<sup>-1</sup> and 1631.7 cm<sup>-1</sup> are attributed to the C=O and C=C stretching vibrations, suggesting the presence of terpenoids and flavonoids. The peaks at 1120.6 cm<sup>-1</sup> and 1066.6 cm<sup>-1</sup> are associated with carboxylic acids, esters, and ether groups, possibly originating from proteins and other metabolites that may function as capping or stabilizing agents [7]. Additionally, a band at 1308 cm<sup>-1</sup> corresponds to C=N stretching of aromatic amines. Weak bands at 983.70 cm<sup>-1</sup>, 700.12 cm<sup>-1</sup>, and 538.04 cm<sup>-1</sup> are assigned to alkenes, alkyl halides (C-Cl), and methoxy (C-OCH<sub>3</sub>) group vibrations, respectively [10].

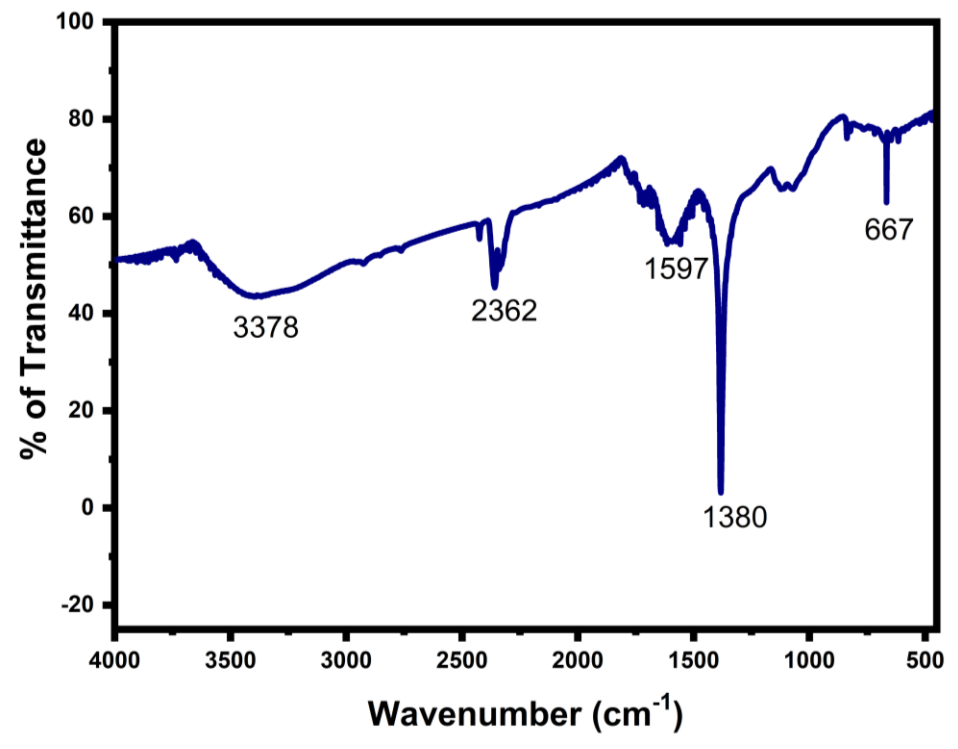


Fig.6: FTIR spectrum of A.marmelos-mediated Ag-NPs

## 3.5 X-ray diffraction analysis of Ag-NPs

X-ray diffraction (XRD) analysis revealed distinct diffraction peaks at 20 values of 38.2°, 43.3°, 64.4° and 77°, corresponding to the (111), (200), (220), and (311) crystallographic planes of metallic silver, respectively (Figure 7). These reflections are characteristic of a face-centered cubic (fcc) structure, consistent with the standard Joint Committee on Powder Diffraction Standards (JCPDS) file No. 03-0921. The sharp and clear peaks confirm the crystalline nature of the synthesized AgNPs, corroborating previous findings [12]. The average crystallite size (S) of the AgNPs, calculated using the Debye–Scherrer equation (3), was found to be approximately 49.36 nm.

$$S = \frac{k\lambda}{\beta \cos \theta}$$
 Eq. (3)

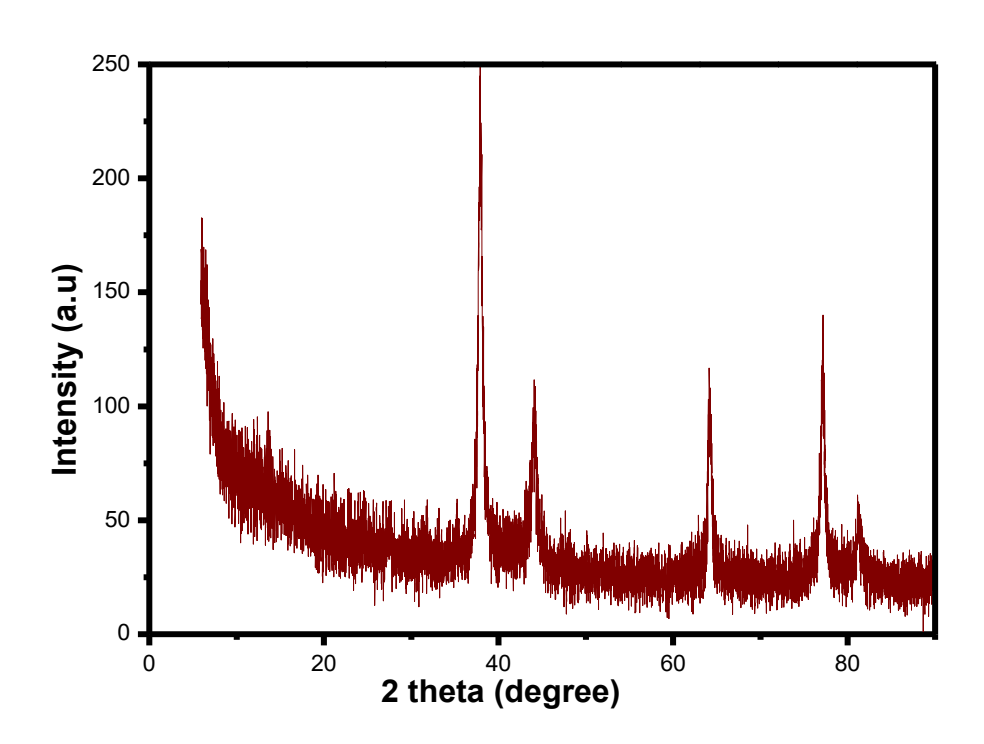


Fig.7: XRD patterns of Ag-NPs synthesized by Aegle marmelos fruit extract **3.6** Antibacterial activity of Ag-NPs

The antibacterial activity of biosynthesized Ag-NPs was evaluated against both Gram-positive and Gram-negative bacteria using the agar well diffusion method. The Ag-NPs synthesized via the green route exhibited significant antibacterial activity against all tested pathogens are Pseudomonas aeruginosa, Corynebacterium glutamicum, Staphylococcus aureus, and Escherichia coli at concentrations of 80, 100, and 150 µg/mL. The results demonstrated a clear dose-dependent antibacterial effect, with increased nanoparticle concentration correlating with larger zones of inhibition. As illustrated in Figure 8, the Ag-NPs were most effective against C.glutamicum, with a maximum zone of inhibition measuring 12.66 ± 0.41 mm at 150 µg/mL. The observed antibacterial effect is likely attributed to the strong affinity of silver ions for thiol groups in essential bacterial respiratory enzymes, disrupting cellular function and leading to microbial death [13]. Overall, the results presented in Figure 8 and Table 3 confirm the potent antibacterial properties of the synthesized Ag-NPs against a broad spectrum of bacterial strains, including Gram-positive (C.glutamicum and S.aureus) and Gram-negative (P. aeruginosa and E.coli) species. The distinct inhibition zones surrounding the wells support the potential of these Ag-NPs as effective and versatile antibacterial agents.

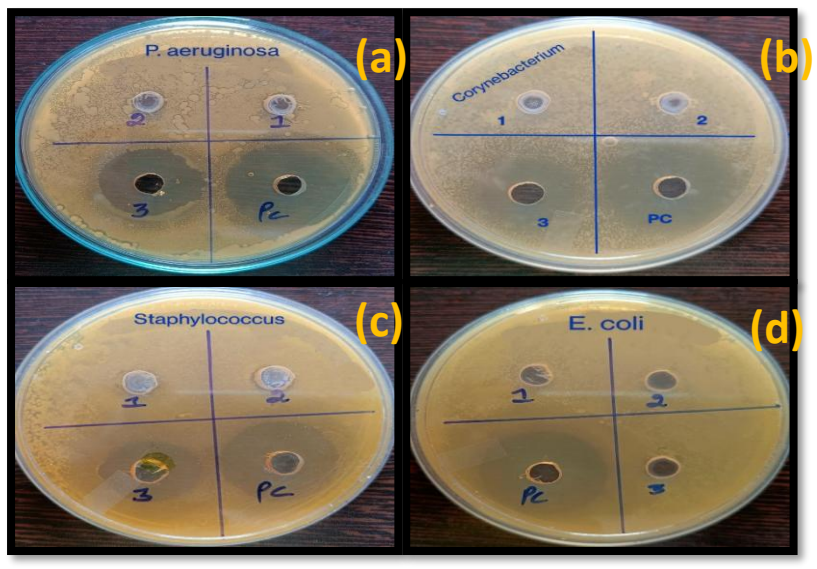


Fig.8: Antibacterial activity of Ag-NPs against (a)P.aeruginosa, (b)C.glutamicum, (c)S.aureus and (d)E.coli

https://theaspd.com/index.php

Table 3: Antibacterial activity of Ag-NPs against bacteria

	Zone of inhibition (mm)					
T	Ag-NPs (	Ag-NPs (μg/mL)				
Test organism	80	100	150	Positive control 30μg/mL		
P.aeruginosa	-	-	11.23±0.63	24.63±1.02		
C.glutamicum	•		12.66±0.41	15.76±1.89		
S.aureus	•	•	10.36±0.22	20.63±1.66		
E.coli	-	-	,	20.73±1.05		

# 3.7 Anticancer activity of Ag-NPs

HCT-116 cell lines were used to assess the anticancer activity of A.marmelos-mediated Ag-NPs, and the outcomes demonstrated the NPs effectiveness. The isolated substance's cytotoxicity in HCT-116 cell lines was measured using the MTT test, and the IC $_{50}$  value was  $41.33\pm0.19~\mu g/mL$  (Table 4). More dead cells were created by increasing the concentration of the purified chemical. A microscopic morphology study of cell lines treated with the isolated material revealed morphological changes (Fig.9). The cells appeared to be constricting and separating from the substrate when observed at x40 magnification using an inverted tissue culture microscope. The flavonoids and polyphenols utilized in their manufacture may have given the nanoparticles cytotoxicity when used against different cancer cell lines, and their smaller size allowed them to very efficiently penetrate the tumor matrix and cancer cells. The anticancer activity might have been influenced by these two elements [20].

Table 4:In-vitro cytotoxicity of Ag-NPs on HCT-116 Cell lines

Ag-NPs (μg/mL)	% Cell viability (HCT 116 cell lines)		
0	100.00		
12.5	66.5±0.51		
25	55.52±0.75		
50	48.70±0.51		
75	36.32±0.05		
100	34.08±0.02		
150	32.60±0.51		
200	29.42±0.03		
$IC_{50}$	41.33±0.19		

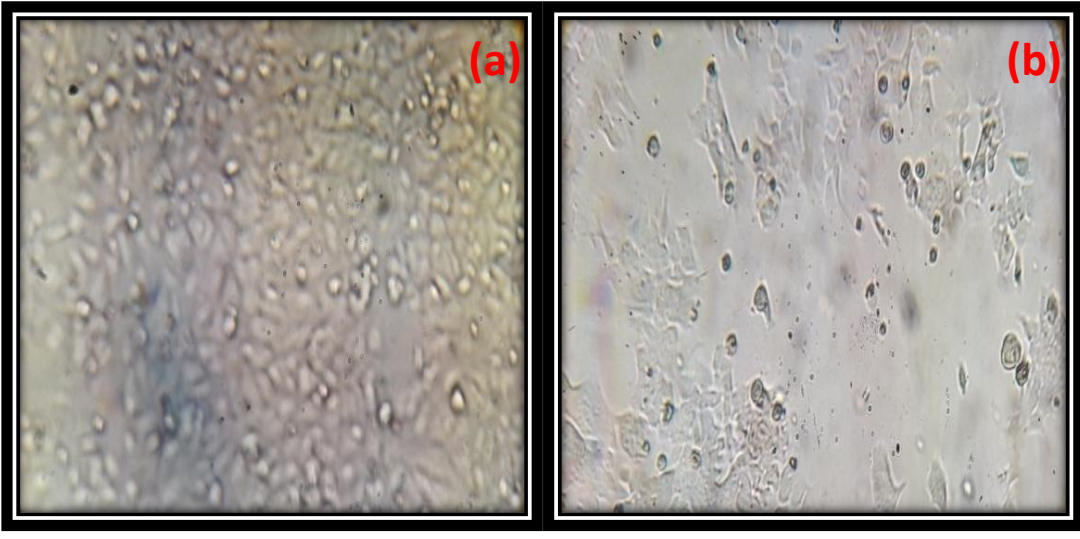


Fig.9: Control and Treatment with Ag-NPs over HCT-116

#### 3.8 Anti-oxidant activity of Ag-NPs

The 2,2-diphenyl-1-picrylhydrazyl (DPPH) assay is based on the reduction of the stable DPPH free radical

to a non-radical form upon receiving an electron or hydrogen atom from an antioxidant molecule [21]. This reduction is accompanied by a color change in the DPPH solution from deep purple to yellow, resulting in decreased absorbance. In the present study, the antioxidant activity of biosynthesized Ag-NPs using A.marmelos fruit extract was evaluated at various concentrations (50, 75, 100, 125, and 150 µg/mL) and compared to ascorbic acid as a standard antioxidant at equivalent concentrations. The Ag-NPs exhibited a maximum antioxidant activity of 85.67% at 100 µg/mL, while the corresponding activity for ascorbic acid at the same concentration was 90.12% (Figure 10). Since oxidative stress caused by free radicals is implicated in the pathogenesis of many human diseases, natural antioxidants are increasingly being explored as safer alternatives to synthetic compounds [5]. Antioxidants play a crucial role in mitigating oxidative damage in cells and have therapeutic potential in managing conditions such as cancer, inflammation, cardiovascular diseases, and respiratory infections [22]. Plant-based antioxidants, including those associated with biogenic Ag-NPs, are gaining attention due to their safety, accessibility, and bioactivity [23, 24]. The synthesized Ag-NPs demonstrated significant antioxidant capacity, highlighting their potential use in preventing or managing oxidative stress-related disorders. These findings are supported by previous studies and comparative evaluations, as summarized in Table 5 [25].

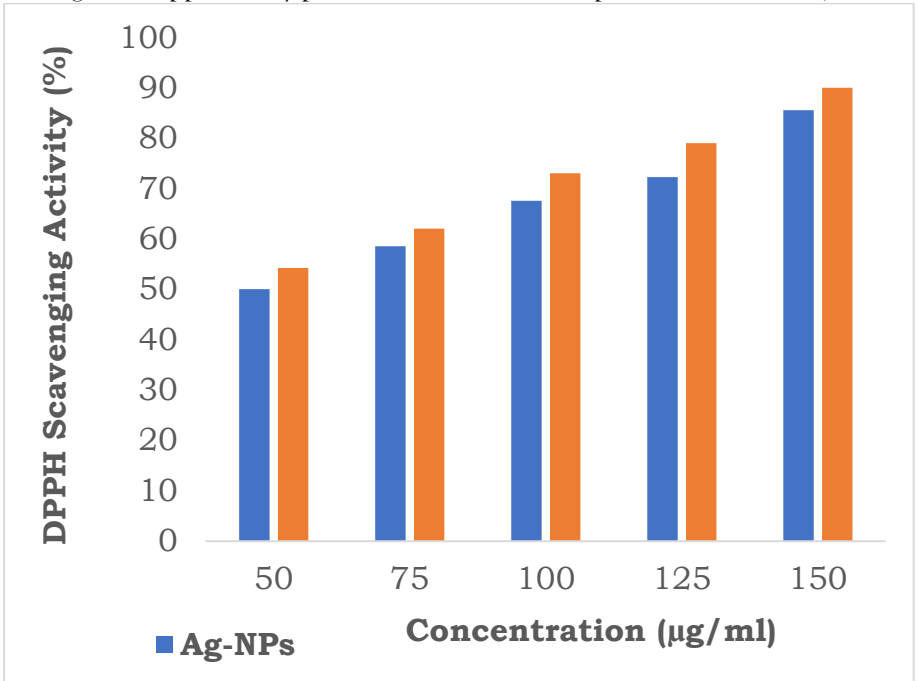


Fig. 10: DPPH radical scavenging activity of Ag-NPs and ascorbic acid Table 5: Antioxidant activity of Ag NPs using various plant fruit extracts

Plant Fruit	Method of	Antioxidant	Results	References
Extract	Synthesis	Assay	Results	References
Lemon	Green synthesis with AgNO <sub>3</sub>	DPPH radical scavenging assay	$IC_{50} = 35 \mu g/mL$	[26]
Grapefruit	Plant-mediated synthesis	Ferric reducing antioxidant power (FRAP) assay	FRAP value = 320 µmol Fe(II)/g extract	[27]
Cranberry	Bio-reduction of Ag+ ions	ABTS radical scavenging assay	$EC_{50} = 25 \mu g/mL$	[28]
Blueberry	Co-precipitation method	Total phenolic content (TPC) assay	TPC = 45 mg GAE/g extract	[29]
Pomegranate	Microwave- assisted synthesis	Oxygen radical absorbance capacity (ORAC) assay	ORAC value = 4800 µmol Trolox equiv/g extract	[30]
A.marmelos	Plant-mediated synthesis	DPPH radical scavenging assay	85.67%	Present study

International Journal of Environmental Sciences

ISSN: 2229-7359 Vol. 11 No. 7, 2025

https://theaspd.com/index.php

#### **CONCLUSION**

In this study, silver nanoparticles (AgNPs) were successfully synthesized using Aegle marmelos fruit extract as a green reducing and stabilizing agent. The formation of AgNPs was visually confirmed by a color change and validated using UV-Vis spectroscopy. The biosynthesized AgNPs demonstrated notable antioxidant activity, with a maximum radical scavenging efficiency of 85.67% at 100 µg/mL, comparable to that of the standard antioxidant ascorbic acid. Moreover, the AgNPs exhibited promising antibacterial properties against both Gram-positive and Gram-negative bacterial strains, including E.coli, P.aeruginosa, S.aureus, and Corynebacterium, as evidenced by significant zones of inhibition in agar well diffusion assays. These findings underline the potential of Aegle marmelos-mediated AgNPs as effective, eco-friendly agents for biomedical applications, particularly in the development of antimicrobial and antioxidant formulations. The study also highlights the advantages of green synthesis methods, contributing to safer and more sustainable nanotechnology. Furthermore, in-vitro and in-vivo research are required to gain a deeper comprehension of Ag-NPs' toxicological characteristics.

#### **Declarations**

## Data availability statement

The data will be provided on request basis to the corresponding author.

#### **Funding**

No funding support

## **Competing Interests**

Authors declare that no conflicts of interest

#### **Author Contributions**

PS: Formal analysis, Data curation, writing-original manuscript; YV: writing-review & editing.

# Ethics approval

Not Applicable

Consent to participate

Not Applicable

## Consent to publish

Not Applicable

# REFERENCES

[1] Anbukkarasi M, Thomas PA, Sundararajan M, Geraldine P. Gas chromatography-mass spectrometry analysis and in vitro antioxidant activity of the ethanolic extract of the leaves of Tabernaemontanadivaricata. Pharm J. 2016; 8:451-458.

[2] Kirubakaran, D., Wahid, J.B.A., Karmegam, N. et al. A Comprehensive Review on the Green Synthesis of Nanoparticles: Advancements in Biomedical and Environmental Applications. Biomedical Materials & Devices (2025). https://doi.org/10.1007/s44174-025-00295-4.

[3] Cameron M, Gagnier J, Little C, Parsons T, Blümle A, Chrubasik S. Evidence of effectiveness of herbal medicinal products in the treatment of arthritis. Part 1: Osteoarthritis. Phytother Res. 2009; 23:1497-1515.

[4] Iravani S, Korbekandi H, Mirmohammadi SV, Zolfaghari B. Synthesis of silver nanoparticles: chemical, physical and biological methods. Res Pharm Sci. 2014; 9:385406.

[5] Khan AK, Rashid R, Murtaza G, Zahra A. Gold nanoparticles: synthesis and applications in drug delivery. Trop J Pharm Res. 2014; 13:1169-1177.

[6] Saini R, Saini S, Sharma S. Nanotechnology: the future medicine. J CutanAesthet Surg. 2010; 3:32-33.

[7] Chandrasekara A, Daugelaite J, Shahidi F. DNA scission and LDL cholesterol oxidation inhibition and antioxidant activities of Bael (Aegle marmelos) flower extracts. J TraditComplemen Med; 2018. https://doi.org/10.1016/j.jtcme.2017. 08.010.

[8] Bar H, Bhui DK, Sahoo GP, Sarkar P, De SP, Misra A. Green synthesis of silver nanoparticles using latex of Jatropha curcas. Colloids Surf APhysicochemEng Asp. 2009; 339:134-139

[9] Rao JK, Paria S. Green synthesis of silver nanoparticles from aqueous Aegle marmelos leaf extract. Mater Res Bull. 2013; 48:628-634.

[10] N. Muniyappan and N. S. Nagarajan, Green synthesis of silver nanoparticles with Dalbergia spinosa leaves and their applications in biological and catalytic activities, Process Biochemistry, vol. 49, no. 6, pp. 1054–1061, 2014.

[11] PSRV Sagar, D Ramadevi, K Basavaiah, SM Botsa. Green synthesis of silver nanoparticles using aqueous leaf extract of Saussureaobvallata for efficient catalytic reduction of nitrophenol, antioxidant, and antibacterial activity. Water Science and Engineering, 2024, 17 (3), 274-282.

[12] Bar, H., Bhui, D. K., Sahoo, G. P., Sarkar, P., De, S. P., & Misra, A. (2009). Green synthesis of silver nanoparticles using latex of Jatropha curcas. Colloids and Surfaces A: Physicochemical and Engineering Aspects, 339(1-3), 134-139.

[13] SM Botsa, K Basavaiah. Fabrication of multifunctional TANI/Cu<sub>2</sub>O/Ag nanocomposite for environmental abatement. Scientific reports, 2020, 10(1), 14080.

[14] C. Krishnaraj, E. G. Jagan, S. Rajasekar, P. Selvakumar, P. T. Kalaichelvan, and N. Mohan, Synthesis of silver nanoparticles using Acalypha indica leaf extracts and its antibacterial activity against water borne pathogens, Colloids and Surfaces B: Biointerfaces, vol. 76, no. 1, pp. 50–56, 2010.

International Journal of Environmental Sciences

ISSN: 2229-7359 Vol. 11 No. 7, 2025

https://theaspd.com/index.php

- [15] Kumar, A., Pant, S., & Kumar, P. (2017). Biosynthesis of silver nanoparticles using Aegle marmelos (Bael) fruit extract: Antioxidant and antimicrobial activities. Journal of Advanced Nanomaterials, 2(4), 25-32.
- [16] Sharma, V. K., Yngard, R. A., & Lin, Y. (2019). Green synthesis of gold nanoparticles using Aegle marmelos fruit extract and their catalytic activity. Materials Research Bulletin, 45(10), 1605-1610.
- [17] Gupta, M., Tomar, R. S., & Kaushik, S. (2020). Synthesis of zinc oxide nanoparticles using Aegle marmelos fruit extract: UV-blocking and antibacterial activities. Journal of Photochemistry and Photobiology B: Biology, 101(3), 209-215.
- [18] Singh, R. P., Dhanjal, D. S., & Verma, N. (2021). Green synthesis of copper nanoparticles using Aegle marmelos fruit extract and their biological activities. Environmental Nanotechnology, Monitoring & Management, 5(2), 190-198.
- [19] J. Kasthuri, S. Veerapandian, and N. Rajendiran, Biological synthesis of silver and gold nanoparticles using apiin as reducing agent, Colloids and Surfaces B: Biointerfaces, vol. 68, no. 1, pp. 55-60, 2009
- [20] Rajkumar, M., Presley, S.I.D., Govindaraj, P.Synthesis of chitosan/PVA/copper oxide nanocomposite using Anacardium occidentale extract and evaluating its antioxidant, antibacterial, anti-inflammatory and cytotoxic activities. Sci Rep., 2025, 15, 3931.
- [21] Abdel-Aziz, M.S.; Shaheen, M.S.; El-Nekeety, A.A.; Abdel-Wahhab, M.A. Antioxidant and antibacterial activity of silver nanoparticles biosynthesized using Chenopodium murale leaf extract. J. Saudi Chem. Soc. 2014, 18, 356–363.
- [22] Hasan, M.; Mehmood, K.; Mustafa, G.; Zafar, A.; Tariq, T.; Hassan, S.G.; Loomba, S.; Zia, M.; Mazher, A.; Mahmood, N.; et al. Phytotoxic evaluation of phytosynthesized silver nanoparticles on lettuce. Coatings, 2021, 11, 225.
- [23] Yin, L.; Cheng, Y.; Espinasse, B.; Colman, B.P.; Auffan, M.; Wiesner, M.; Rose, J.; Liu, J.; Bernhardt, E.S. More than the ions: The effects of silver nanoparticles on Lolium multiflorum. Environ. Sci. Technol. 2011, 45, 2360–2367.
- [24] Singh, N., Pandey, S., Dubey, S., Antioxidant and cytotoxic activities of gold nanoparticles synthesized from blueberry fruit extract. Journal of Nanostructure in Chemistry, 2018, 8(4), 379-389.
- [25] Saravanan, M.; Barik, S.K.; MubarakAli, D.; Prakash, P.; Pugazhendhi, A. Synthesis of silver nanoparticles from Bacillus brevis (NCIM 2533) and their antibacterial activity against pathogenic bacteria. Microb. Pathog. 2018, 116, 221–226.
- [26] Gan, P. P., & Li, S. F. Y. Green synthesis of gold nanoparticles using Palm oil mill effluent (POME): A low-cost sustainable bio-resource. Industrial Crops and Products, 2012, 37(1), 284-289.
- [27] Chen, Y., Li, M., Zhang, Y., & Yu, L. Biofabrication of silver nanoparticles using grapefruit peel extract for applications in catalysis and antibacterial activity. Journal of Applied Polymer Science, 2019, 136(13), 1-8.
- [28] Ahmad, N., Sharma, S., Singh, V. N., Shamsi, S. F., Fatma, A., & Mehta, B. R. Biosynthesis of silver nanoparticles from Desmodiumtriflorum: A novel approach towards weed utilization. Biotechnology Research International, 2011, 2011, 454090. [29] Shankar, S. S., Rai, A., Ahmad, A., & Sastry, M. Rapid synthesis of Au, Ag, and bimetallic Au core–Ag shell nanoparticles using Neem (Azadirachta indica) leaf broth. Journal of Colloid and Interface Science, 2011, 275(2), 496-502.
- [30] MS Mohseni, MA Khalilzadeh, M Mohseni, FZ Hargalani, MI Getso, V Raissi, O Raiesi. Green synthesis of Ag nanoparticles from pomegranate seeds extract and synthesis of Ag-Starch nanocomposite and characterization of mechanical properties of the films. Biocatalysis and Agricultural Biotechnology, 2020, 25, 101569.